

# Kerr Geodesics, the Penrose Process and Jet Collimation by a Black Hole

J. Gariel<sup>1\*</sup>, M. A. H. MacCallum<sup>2†</sup>, G. Marcilhacy<sup>1‡</sup> and N. O. Santos<sup>2,3§</sup>

<sup>1</sup>Université Pierre et Marie Curie - CNRS/UMR 8112,

LERMA/ERGA, Boîte 142, 4 place Jussieu, 75252 Paris Cedex 05, France.

<sup>2</sup>School of Mathematical Sciences, Queen Mary,

University of London, London E1 4NS, UK.

<sup>3</sup>Laboratório Nacional de Computação Científica,

25651-070 Petrópolis RJ, Brazil.

April 23, 2019

## Abstract

We re-examine the possibility that astrophysical jet collimation may arise from the geometry of rotating black holes and the presence of high-energy particles resulting from a Penrose (or similar) process without the help of magnetic fields. Our analysis uses Weyl coordinates, which are better adapted to the shape of the jets, and provides insight into a number of features of the mechanism, such as the expected size and internal structure of such jets.

## 1 Introduction

There is increasing evidence (McKinney, 2005) that a single mechanism is at work in the production and collimation of various very energetic observed jets, such as those in gamma ray bursts (GRB) (Piran et al., 2001;

---

\*E-mail: gariel@ccr.jussieu.fr

†E-mail: M.A.H.MacCallum@qmul.ac.uk

‡E-mail: gmarcilmacy@hotmail.com

§E-mail: N.O.Santos@qmul.ac.uk

Sheth et al., 2003; Fargion, 2003), and jets ejected from active galactic nuclei (AGN) (Sauty et al., 2002) and from microquasars (Mirabel & Rodriguez, 1994, 1999). Here we limit ourselves to jets produced by a black hole (BH) type core. The most often invoked process is the Blandford-Znajek (Blandford & Znajek, 1977) or some closely similar mechanism (e.g. Punsly & Coroniti (1990a,b); Punsly (2001)) in the framework of magnetohydrodynamics, always requiring a magnetic field. However such mechanisms are limited to charged particles, and would be inefficient for neutral particles (neutrons, neutrinos and photons), which are currently the presumed antecedents of very thin and long duration GRB (Fargion, 2003). Moreover, even for charged particles, some questions persist (see for instance the conclusion of Williams (2004)). Finally, while the observations of synchrotron radiation prove the presence of magnetic fields, they do not prove that those fields alone cause the collimation: magnetic mechanisms may be only a part of a more unified mechanism for explaining the origin and collimation of powerful jets, see Livio (1999) p. 234 and section 5, and, in particular, for collimation of jets from AGN to subparsec scales, see de Felice & Zanotti (2000).

Considering this background, it is worthwhile looking for other types of model to explain the origin and structure of jets. Other models based on a purely general relativistic origin for jets have been considered. A simple model was obtained by Opher et al. (1996) by assuming the centres of galaxies are described by a cylindrical rotating dust. They showed that confinement occurs in the radial motion of test particles while the particles are accelerated in the axial direction thus producing jets. Another relativistic model was put forward by Herrera & Santos (2005). They showed that the sign of the proper acceleration of test particles near the axis of symmetry of quasi-spherical objects and close to the horizon can change. This outward acceleration, that can be very big, might cause the production of jets.

However, these models show a powerful gravitational effect of repulsion only near the axis, and are built in the framework of axisymmetric stationary metrics which do not have an asymptotic behaviour compatible with possible far away observations. So we want to explore the more realistic rotating black hole, i.e. Kerr, metrics instead.

We address here the issue of whether it is possible, at least in principle (i.e. theoretically) to obtain a very energetic and perfectly collimated jet without making use of magnetic fields. Other authors (see Williams (1995, 2004); de Felice & Carlotto (1997) and references therein) have made related studies to which we refer below. Most such authors agree that the strong

gravitational field generated by rotating BHs is essential to understanding the origin of jets; more precisely, that the jet originates from a Penrose-like process (Penrose, 1969; Williams, 2004) in the ergosphere of the BH. Collimation also arises from the gravitational field and this is the main topic in this paper.

From a strictly general relativistic point of view, test particles in vacuum (here, a Kerr spacetime) follow geodesics (though of course in an electrovacuum spacetime, such as Kerr-Newman, charged particles would follow accelerated trajectories). Thus what produces an eventual collimation for test particles, or not, is the form of the resulting geodesics. Hence we discuss here the possibilities of forming an outgoing jet of collimated geodesics followed by particles arising from a Penrose-like process inside the ergosphere of a Kerr BH. We show that it is possible to obtain such a jet from a purely gravitational model.

The model is based on the following considerations.

Most studies of geodesics, e.g. Chandrasekhar (1983), employ generalized spherical, i.e. Boyer-Lindquist, coordinates. We transform to Weyl coordinates, which are generalized cylindrical coordinates, and are more appropriate, as we shall see, for interpreting the collimated jets.

We consider (uncharged) test particles moving in the axisymmetric stationary gravitational field produced by the Kerr spacetime, whose geodesic equations, as projected into a meridional plane, are known (Chandrasekhar, 1983). Our study is restricted to massive test particles, moving on timelike geodesics, but of course massless test particles on null geodesics could be the subject of a similar study.

For particles outgoing from the ergosphere of the Kerr BH we examine their asymptotic behaviour. Among the geodesic particles incoming to the ergosphere, we consider only the ones coming from infinity parallel to the equatorial plane. Infinity means in practice particles stemming from the accretion disk.

In the ergosphere, a Penrose-like process can occur. In the original Penrose process, an incoming particle decays into two parts inside the ergosphere. It could also decay into more than two parts, or undergo a collision with another particle in this region, or give rise to pair creation ( $e^-, e^+$ ) from incident photons which would follow null geodesics. The different possible cases do not change the essentials of our results, and that is why we do not study them here, although the distribution function of outgoing particles would be required in a more detailed model. For detailed studies see Williams (1995,

2004); Piran & Shaham (1977). After the decay, one of the particles produced crosses the event horizon and irreversibly plunges into the BH, while a second particle arising from the decay can be ejected out of the ergosphere following a geodesic towards infinity. If such a path is possible this outgoing particle could be asymptotically ejected parallel to the axis of symmetry, but we do not discuss only such particles.

In our model there is no appeal to electromagnetic forces to explain the ejection or the collimation of jets. The gravitational field suffices, in the case of strong fields in general relativity, which is the case near the Kerr BH. The gravitomagnetic part of the gravitational field drives the collimation. Hence, our model is, in this respect, simpler than the standard model of Blandford & Znajek (1977), and is in accordance with the analysis given in Williams (2004).

The paper starts with a study of Kerr geodesics in Weyl coordinates in section 2; the next section studies the geodesics of asymptotically outgoing particles from the Kerr ergosphere; section 4 analyses incoming particles stemming from the accretion disk; section 5 gives further remarks about incoming and outgoing particles; a sample Penrose process and the plotting of geodesics are presented in section 6. In the conclusion, we succinctly summarize our main results and evoke some perspectives.

## 2 Kerr geodesics

We start from the projection in a meridional plane  $\phi = \text{constant}$  of the Kerr geodesics in Boyer-Lindquist spherical coordinates  $r, \theta$  and  $\phi$ . The metric is

$$\begin{aligned} ds^2 = & (\bar{r}^2 + a^2 \cos^2 \theta) \left( \frac{d\bar{r}^2}{\bar{r}^2 - 2M\bar{r} + a^2} + d\theta^2 \right) \\ & + \frac{\sin^2 \theta}{(\bar{r}^2 + a^2 \cos^2 \theta)} (adt - (\bar{r}^2 + a^2) d\varphi)^2 \\ & - \frac{(\bar{r}^2 - 2M\bar{r} + a^2)}{(\bar{r}^2 + a^2 \cos^2 \theta)} (dt - a \sin^2 \theta d\varphi)^2. \end{aligned} \quad (1)$$

where  $M$  and  $Ma$  are, respectively, the mass and the angular momentum of the source, and we have taken units such that  $c = 1 = G$  where  $G$  is Newton's constant of gravitation. The 'radial' coordinate in (1) has been named  $\bar{r}$  because it is more convenient for us to use the rescaled coordinate

$r = \bar{r}/M$  (O'Neill, 1995). The projected timelike geodesic equations are then

$$M^2 \dot{r}^2 = \frac{(a_4 r^4 + a_3 r^3 + a_2 r^2 + a_1 r + a_0)}{\left[ r^2 + \left( \frac{a}{M} \right)^2 \cos^2 \theta \right]^2}, \quad (2)$$

$$M^2 \dot{\theta}^2 = \frac{b_4 \cos^4 \theta + b_2 \cos^2 \theta + b_0}{(1 - \cos^2 \theta) \left[ r^2 + \left( \frac{a}{M} \right)^2 \cos^2 \theta \right]^2}, \quad (3)$$

with coefficients

$$a_0 = -\frac{a^2 \mathcal{Q}}{M^4}, \quad (4)$$

$$a_1 = \frac{2}{M^2} [(aE - L_z)^2 + \mathcal{Q}], \quad (5)$$

$$a_2 = \frac{1}{M^2} [a^2(E^2 - 1) - L_z^2 - \mathcal{Q}], \quad (6)$$

$$a_3 = 2, \quad (7)$$

$$a_4 = E^2 - 1, \quad (8)$$

and

$$b_0 = \frac{\mathcal{Q}}{M^2}, \quad (9)$$

$$b_2 = \frac{1}{M^2} [a^2(E^2 - 1) - L_z^2 - \mathcal{Q}] = a_2, \quad (10)$$

$$b_4 = -\left( \frac{a}{M} \right)^2 (E^2 - 1); \quad (11)$$

where the dot stands for differentiation with respect to an affine parameter and  $E$ ,  $L_z$  and  $\mathcal{Q}$  are constants. Here Chandrasekhar's  $\delta_1$  has been set to 1, its value for timelike curves. Assuming that the affine parameter is proper time  $\tau$  along the geodesics, then these equations implicitly assume a unit mass for the test particle<sup>1</sup>, so that  $E$  and  $L_z$  have the usual significance of total energy and angular momentum about the  $z$ -axis, and  $\mathcal{Q}$  is the corresponding Carter constant (which, as described in Hughston et al. (1972) for example, arises from a Killing tensor of the metric, while  $E$  and  $L_z$  arise from Killing vectors). With this understanding,  $E$ ,  $L_z$ , and  $\mathcal{Q}$  have the dimensions of

---

<sup>1</sup>An alternative interpretation is to assume that for a particle of mass  $m$ , the affine parameter  $\tau/m$  has been used (Wilkins, 1972; Williams, 1995).

Mass,  $\text{Mass}^2$  and  $\text{Mass}^4$  respectively, in geometrized units, while  $\delta_1$ , though 1 numerically, has dimensions  $\text{Mass}^2$ , as do all the  $a_i$  and  $b_i$ . In this paper we consider only particles on unbound geodesics with  $E \geq 1$ . (For the conditions for existence of a turning point, related to the parameter values for associated circular orbits, see Chandrasekhar (1983); Williams (1995, 2004).)

The dimensionless Weyl cylindrical coordinates, in multiples of geometrical units of mass  $M$ , are given by

$$\rho = [(r-1)^2 - A]^{1/2} \sin \theta, \quad z = (r-1) \cos \theta, \quad (12)$$

where

$$A = 1 - \left(\frac{a}{M}\right)^2. \quad (13)$$

From (12) we have the inverse transformation

$$r = \alpha + 1, \quad (14)$$

$$\sin \theta = \frac{\rho}{(\alpha^2 - A)^{1/2}}, \quad \cos \theta = \frac{z}{\alpha}, \quad (15)$$

with

$$\alpha = \frac{1}{\sqrt{2}} \left\{ \rho^2 + z^2 + A + [(\rho^2 - z^2 + A)^2 + 4\rho^2 z^2]^{1/2} \right\}^{1/2}, \quad (16)$$

by assuming  $A \geq 0$ , and taking the root of the second degree equation obtained from (15) for the function  $\alpha^2(\rho, z)$  that allows the extreme black hole limit  $A = 0$ . The other root, in this limit, is the constant  $\alpha = 0$ .

Now, with (14) and (15) we can write the geodesics (2) and (3) in terms of  $\rho$  and  $z$  coordinates, producing the following autonomous system of first order equations

$$M\dot{\rho} = \epsilon_1 \frac{\frac{P\alpha^3\rho}{\alpha^2 - A} + \frac{S(\alpha^2 - A)z}{\alpha\rho}}{(\alpha + 1)^2\alpha^2 + \left(\frac{a}{M}\right)^2 z^2}, \quad (17)$$

$$M\dot{z} = \epsilon_2 (Pz - S)\alpha \left[ (\alpha + 1)^2\alpha^2 + \left(\frac{a}{M}\right)^2 z^2 \right]^{-1}, \quad (18)$$

where (understanding that we always take positive square roots)

$$P = [a_4(\alpha + 1)^4 + a_3(\alpha + 1)^3 + a_2(\alpha + 1)^2 + a_1(\alpha + 1) + a_0]^{1/2}, \quad (19)$$

$$S = \epsilon_3 (b_4 z^4 + b_2 \alpha^2 z^2 + b_0 \alpha^4)^{1/2}, \quad (20)$$

and  $\epsilon_i = \pm 1$  for  $i = 1, 2, 3$ .

The ratio between the first order differential equations (17) and (18) yields the special characteristic equation of this system of equations

$$\frac{dz}{d\rho} = \epsilon_1 \epsilon_2 \frac{(Pz - S)(\alpha^2 - A)\alpha^2 \rho}{P\alpha^4 \rho^2 + S(\alpha^2 - A)^2 z}. \quad (21)$$

For  $\rho \gg z$  we have from (21)

$$\frac{dz}{d\rho} \approx \epsilon_1 \epsilon_2 \frac{z - \epsilon_3 z_1}{\rho} + O(\rho^{-2}), \quad (22)$$

where

$$z_1 = \left( \frac{b_0}{a_4} \right)^{1/2} = \frac{1}{M} \left( \frac{\mathcal{Q}}{E^2 - 1} \right)^{1/2}, \quad (23)$$

and we have to assume  $\mathcal{Q} \geq 0$  to obtain a real  $z_1$  (the form of (3) makes it obvious that geodesics with  $\mathcal{Q} < 0$  are bounded away from the equatorial plane  $\cos \theta = 0$ , though those with very small  $|\mathcal{Q}|$  could still satisfy  $\rho \gg z$ ).

For  $z \gg \rho$  we first observe that from (20) we have

$$S \approx \epsilon_3 [(b_0 + b_2 + b_4)z^4 + (2b_0 + b_2)\rho^2 z^2]^{1/2} + O(z^{-1}), \quad (24)$$

where

$$b_0 + b_2 + b_4 = - \left( \frac{L_z}{M} \right)^2 \leq 0, \quad (25)$$

$$2b_0 + b_2 = \frac{1}{M^2} [a^2(E^2 - 1) - L_z^2 + \mathcal{Q}]. \quad (26)$$

Hence in this limit  $S$  is well defined and real for indefinitely small  $\rho/z$  only for  $L_z = 0$ .

The geodesics (21) in this limit ( $L_z = 0$ ,  $z \gg \rho$ ) obey the equation

$$\frac{dz}{d\rho} \approx \frac{\epsilon_1 \epsilon_2 z}{\rho + \epsilon_3 \rho_1} + O(z^{-1}), \quad (27)$$

where

$$\rho_1 = \left( \frac{2b_0 + b_2}{a_4} \right)^{1/2} = \frac{1}{M} \left( a^2 + \frac{\mathcal{Q}}{E^2 - 1} \right)^{1/2}, \quad (28)$$

which is real if  $a^2(E^2 - 1) + \mathcal{Q} > 0$ .

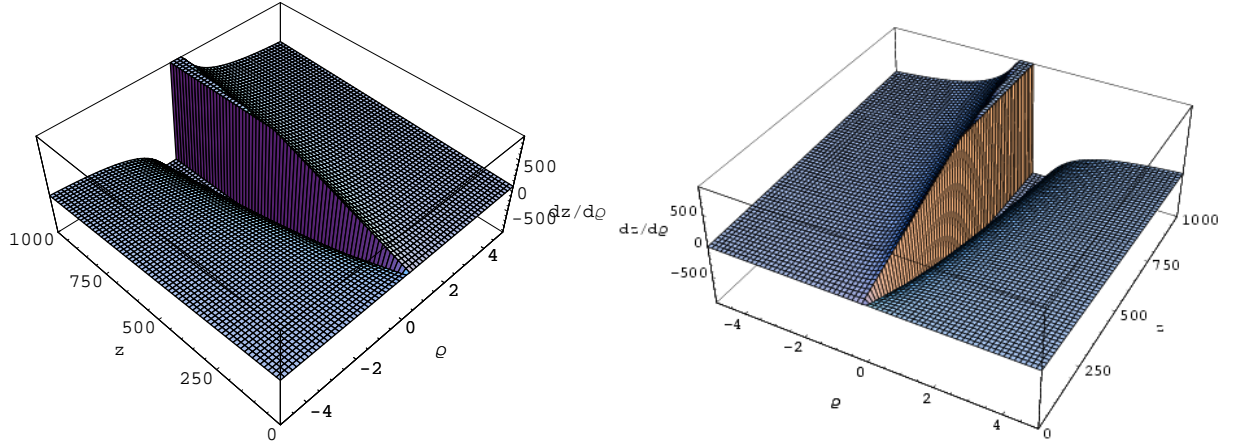


Figure 1: Plot of the surface  $dz/d\rho = f(\rho, z)$  given by equation (21) for an outgoing particle with the parameters  $E = 10^4$ ,  $L_z = 0$  and  $\mathcal{Q} = -9 \times 10^3$  for a black hole with parameters  $M = 1$  and  $a = 0.5$ , in the case where  $\epsilon_3 = 1$  and  $\epsilon_1\epsilon_2 = 1$  (upper plot) and  $\epsilon_1\epsilon_2 = -1$  (lower plot). The points where  $dz/d\rho \rightarrow \infty$  correspond to the asymptote given by the equation  $\rho = 0$ .

Using (21) we have plotted the surfaces  $dz/d\rho = f(\rho, z)$  for the two possible cases  $\epsilon_3 = +1$  and  $\epsilon_3 = -1$ , with the same values of the parameters ( $M = 1$ ,  $a = 1/2$ ,  $E = 10^4$ ,  $\mathcal{Q} = -9 \times 10^3$ ). In the first case, the only asymptote is the equatorial plane  $\rho = 0$  (see Figs. 1). In the second case, the only asymptotes are the parallels to the  $z$  axis  $\rho = \rho_1$  as expected from (27) (see Figs. 2).

We call the particles with  $L_z = 0$  and  $z \gg \rho$  which follow the geodesics (21) with asymptotic conditions given by (27), whence  $|dz/d\rho| \rightarrow \infty$ , type I; while those with asymptotic condition (22), when  $|dz/d\rho| \rightarrow 0$  for  $\rho \gg z$ , are called type II. We may note that in contrast to geodesics with  $L_z \neq 0$ , geodesics with  $E^2 > 1$  and  $L_z = 0$  may lie arbitrarily close to the polar axis whatever the value of  $\mathcal{Q}$  (Carter, 1968) (for  $L_z \neq 0$ , those with  $\mathcal{Q} > 0$  can take any value of  $\theta$  but those with  $\mathcal{Q} < 0$  are restricted to some range  $0 < \cos^2 \theta_0 \leq \cos^2 \theta \leq 1$ ).

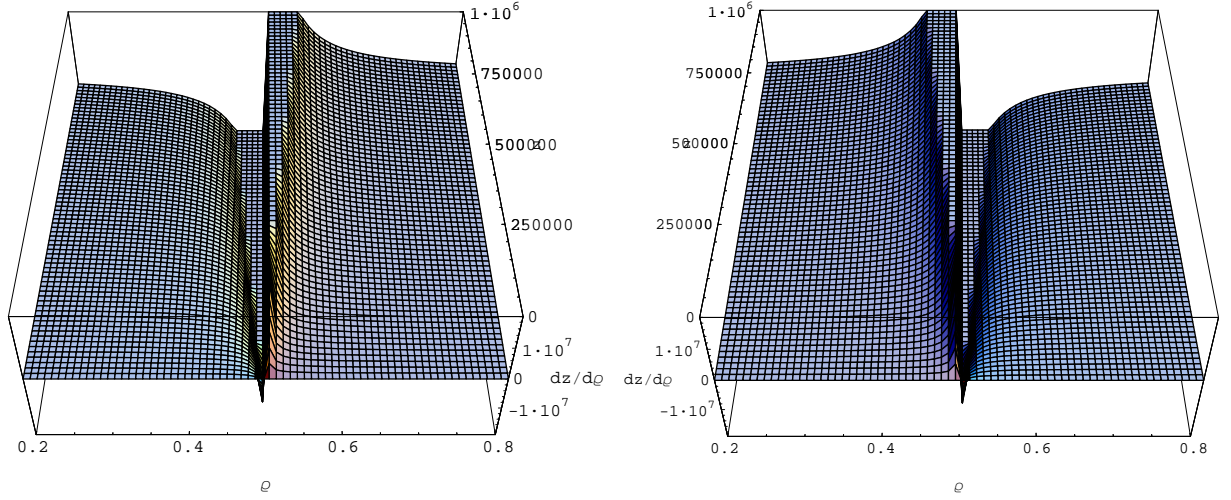


Figure 2: Plot of the surface  $dz/d\rho = f(\rho, z)$  given by equation (21) for an outgoing particle with the parameters  $E = 10^4$ ,  $L_z = 0$  and  $\mathcal{Q} = -9 \times 10^3$  for a black hole with parameters  $M = 1$  and  $a = 0.5$ , in the case where  $\epsilon_3 = -1$  and  $\epsilon_1\epsilon_2 = 1$  (upper plot) and  $\epsilon_1\epsilon_2 = -1$  (lower plot). The points where  $dz/d\rho \rightarrow \pm\infty$  correspond to the asymptotes given by the equation (29),  $\rho = \rho_1 = 0.49991$ .

### 3 Outgoing particles

We want to study particles asymptotically ejected along lines parallel to the  $z$  axis, which we call outgoing particles. We restrict our study to the quadrant  $\rho > 0$  and  $z > 0$  in the plane given by  $\phi = \text{constant}$ . By symmetry, the results will be similar in the other three quadrants. (However this does not exclude the existence of geodesics asymmetric with respect to the equatorial plane. From numerical solutions of the geodesics we obtained asymmetrical geodesics, confirming the analysis in Williams (1995, 2004).) Such particles are the aforesaid type I with asymptotes (28), i.e.

$$\rho_1 = \rho_e \left[ 1 + \frac{\mathcal{Q}}{a^2(E^2 - 1)} \right]^{1/2}, \quad (29)$$

with

$$\rho_e = \frac{a}{M}, \quad (30)$$

and we saw that, in this case, the single possible type of geodesic corresponds to particles with zero angular momentum  $L_z = 0$ . Moreover, if  $\mathcal{Q} < 0$ , then (29) imposes  $a > [|\mathcal{Q}|/(E^2 - 1)]^{1/2}$ .

Asymptotically for type I particles in  $z \gg \rho$  we have from (17)  $\dot{\rho} \rightarrow 0$ ,  $t \rightarrow E$  and (18) is given by

$$M\dot{z} \approx \epsilon_2 \sqrt{a_4}; \quad (31)$$

hence, restoring normal units of length and time and taking a particle of mass  $m$ , the asymptotic value  $v$  of the speed of outgoing particles is given by

$$mM|\dot{z}| \approx \left( \frac{E^2}{c^4} - m^2 \right)^{1/2} = m\gamma \frac{v}{c}, \quad (32)$$

where we have used (8) and

$$\gamma = \left[ 1 - \left( \frac{v}{c} \right)^2 \right]^{-1/2} = \frac{E}{mc^2}, \quad (33)$$

is the Lorentz factor. Hence, asymptotically, the speed of the particle is

$$v = c \frac{M\dot{z}}{t} = c \left( 1 - \frac{m^2 c^4}{E^2} \right)^{1/2}, \quad (34)$$

which is ultrarelativistic if  $E \gg \sqrt{mc^2}$ . From (32) we have that asymptotically outgoing particles have an uniform motion parallel to the  $z$  axis.

There are two kinds of outgoing Type I particles of interest which are the following.

### 3.1 Particles with $\rho < \rho_1$

In this case (17) and (18) imply that  $\dot{z} > 0$  always, and that  $\dot{\rho} > 0$  if  $Sz(\alpha^2 - A^2) > -\alpha^2 P \rho^2$ , this condition always being satisfied in the limit  $z \gg \rho$  if  $\rho < \rho_1$ . Then (27) produces

$$\frac{dz}{d\rho} \approx \frac{z}{\rho_1 - \rho}, \quad (35)$$

in the limit  $z \gg \rho$  for  $\forall \rho$  such that  $0 < \rho < \rho_1$  and  $\forall z > 0$ . In this limit  $dz/d\rho$  tends towards  $+\infty$  when  $\rho \rightarrow \rho_1$ . Each ascending particle asymptotically tends towards a line parallel to the  $z$  axis with equation  $\rho = \rho_1$  from its left. There are as many asymptotes as there are possible values of  $\rho_1$  and the jet contains the set of geodesics with these asymptotes. To each geodesic corresponds so-called outgoing particles defined by their parameters  $E$ ,  $L_z = 0$  and  $\mathcal{Q}$  which are ejected when  $z \gg \rho$  towards the asymptote  $\rho = \rho_1$  (see Fig. 3, which shows an outgoing geodesic (dashed curve) asymptotic to  $\rho = \rho_1$  with  $\rho < \rho_1$ ).

From (29) we can see that very energetic outgoing particles, such that  $E^2 \gg (|\mathcal{Q}|/a^2)$  and 1, are ejected asymptotically in the direction  $\rho_1 \approx \rho_e$ . On the other hand, outgoing particles with small energies, namely of the order of their rest energy,  $E \approx 1$ , and  $\mathcal{Q} > 0$  have asymptotes parallel to the  $z$  axis with  $\rho_1 \gg \rho_e$ . It is worth noting that  $\rho = \rho_e$ ,  $z = 0$  is the circumference of the ergosphere in the equatorial plane, so only geodesics such that  $\rho < \rho_e$  as  $z \rightarrow 0$  can come from inside the ergosphere, and hence only particles on such geodesics can have arisen from a Penrose-like process. This predicted scale might provide a test of our model if the accretion disk parameters provided values for the BH mass and angular momentum, in a manner such as discussed in McClintock et al. (2006) and papers cited therein, and if the transverse linear scale of the jet near the BH could be measured.

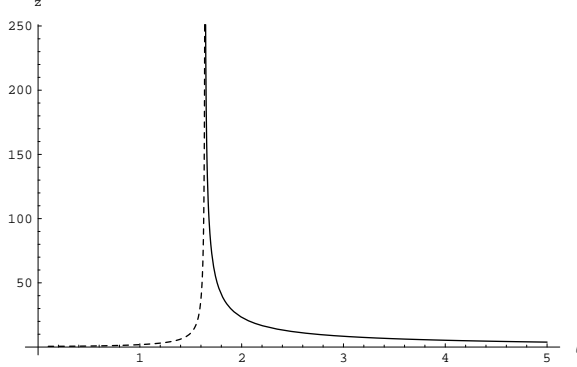


Figure 3: The collimation process. Plots of geodesics tending asymptotically, for  $z \rightarrow \infty$ , towards the asymptote  $\rho = \rho_1 = 1.64341$ , from its left or from its right, for the following values of parameters  $E = 202$ ,  $L_z = 0$  and  $Q = 100000$ ,  $\epsilon_3 = -1$  with  $\epsilon_1\epsilon_2 = -1$  for the dashed curve and  $\epsilon_1\epsilon_2 = 1$  for the full curve.

### 3.2 Particles with $\rho > \rho_1$

In this case (27) is better written as

$$\frac{dz}{d\rho} \approx -\frac{z}{\rho - \rho_1}, \quad (36)$$

in the limit  $z \gg \rho$  for  $\forall \rho > \rho_1$ . Now from (17) and (18) we have  $\dot{\rho} < 0$  and  $\dot{z} > 0$  which means that the ascending geodesics approach the asymptote from its right (see the full curve in Fig. 3). Such outgoing particles can cross the ergosphere, and so may be produced by a Penrose-like process, only if  $\rho_1 \leq \rho_e$ , which corresponds to the case  $Q < 0$ , see (29), since otherwise the particles always have  $\rho > \rho_1 > \rho_e$  which means they are beyond the maximum radius of the ergosphere. When  $\rho_1 < \rho_e$ , such geodesics would also contribute to the jet and reinforce it. The jet would be more intense, since there could be contributions from right and left of  $\rho_1$  by sufficiently energetic particles when  $\rho_1 < \rho_e$ . On the other hand, when  $\rho_1 > \rho_e$ , geodesics with  $\rho > \rho_1$  can never come from the ergoregion, so the corresponding particles cannot be the result of a Penrose process, and hence have insufficient energy to contribute significantly to the jet.

From (29), we see that for  $\rho > \rho_1$  particles with large energies  $E^2 \gg (|Q|/a^2)$  and 1, are again ejected asymptotically in the direction  $\rho_1 \approx \rho_e$ ,

but they do not come from the ergoregion if  $\rho_1 \geq \rho_e$ , while particles with the minimum energy  $E = [(|Q|/a^2) + 1]^{1/2}$  correspond to particles moving asymptotically along the  $z$  axis with  $\rho_1 = 0$ .

For a given  $Q$  and if  $\rho_1 \rightarrow \rho_e$  then from (29)  $E$  is large, describing ultrarelativistic particles. If  $Q > 0$  then  $\rho_1 > \rho_e$ , which means that these particles cannot participate in the jet; only the outgoing ones discussed in section 3.1 for which  $\rho < \rho_1$  can. If  $Q < 0$  and  $\rho_1 \leq \rho_e$  then particles which participate in the jets can arise both as described in Section 3.1 and in this section. Hence, if no sign of  $Q$  is favoured by the production process, a larger number of particles can participate in the jet for  $Q < 0$  than for  $Q > 0$ . For both cases, the most energetic particles are those for which  $\rho_1 = \rho_e$ . Consequently, the most intense part of the jet, i.e. the part with the most energetic particles, is expected to be located just inside the ergosphere where  $\rho_1 \lesssim \rho_e$ . We may note also that the jet will be less energetic, and probably less populated, in its core.

## 4 Incoming particles

A test particle with parameters  $E'$ ,  $L'_z$ , and  $Q'$  coming from infinity (in practice from the accretion disk) parallel to the  $\rho$  axis towards the  $z$  axis of the black hole corresponds to a geodesic which, in the limit  $\rho \rightarrow \infty$ , has an asymptote defined by  $z = z_1 = \text{constant}$  where  $z_1$  is the impact parameter. Therefore it is a type II particle with  $z < z_1$ ,  $\dot{z} < 0$ ,  $\dot{\rho} < 0$ ,  $\epsilon_3 = 1$  and  $\epsilon_1 = \epsilon_2 = -1$ . We call it an incoming particle. In the limit  $\rho \gg z$ ,  $dz/d\rho = 0$ , so the tangent has to be parallel to the  $\rho$  axis and (23) produces

$$z_1 = \frac{1}{M} \left( \frac{Q'}{E'^2 - 1} \right)^{1/2}. \quad (37)$$

We have plotted in Fig. 4 (see section 6) an example of a geodesic of an incoming particle. We see that, unlike  $\rho_1$ ,  $z_1$  does not depend upon the black hole parameter  $a$ . The incoming particles come from the accretion disk, which means that their energy  $E'$  is rarely very big, which means *rarely as big as  $a$  or  $M$* , which characterize the black hole energy, but instead of the same order as 1 or  $\sqrt{Q'}$ . When  $E' \rightarrow 1$  then  $z_1 \rightarrow \infty$  if  $Q' \neq 0$ . However, if  $E'$  is very big compared to 1 and  $\sqrt[4]{Q'}$ , then  $z_1 \rightarrow 0$ .

For a given  $Q'$ , the most energetic incoming particles are those with a small impact parameter  $z_1$ , near to zero. The point where the ergosphere

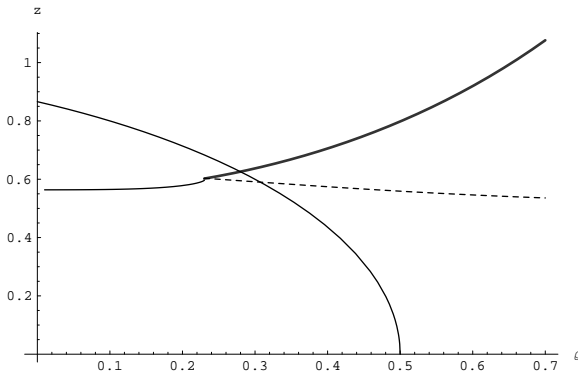


Figure 4: Penrose process. Plots of the ingoing particle (dashed line) coming asymptotically, for  $\rho \rightarrow \infty$ , from  $z_1 = 1.58116$ , at the turning point ( $\rho = 0.23$ ,  $z = 0.59$ ) located inside the ergosphere, whose boundary is indicated, where it decays into an infalling particle and an outgoing particle (bold line) following a geodesic asymptotic to  $\rho = \rho_1 = 1.64341$  when  $z \rightarrow \infty$ . (For the shape of the end of this outgoing geodesic, see the dashed curve in Fig. 3.) The parameters of the black hole are  $M = 1$  and  $a = 0.5$ . The parameters of the three geodesics are  $E_{in} = 200$ ,  $E_{out} = 202$ ,  $E_{fall} = -2$ ,  $L_{z,in} = L_{z,fall} = -100$ ,  $L_{z,out} = 0$ ,  $\mathcal{Q} = \mathcal{Q}' = 100000$ .

surface intersects the axis  $z$  is  $z_e = \sqrt{A}$ . The value of  $z_e$ , for the incoming particles, does not play a role like that of  $\rho_e$  for the outgoing particles (compare (29) to (37)). Hence only a thin slice of the accretion disk can participate with the greatest efficiency in producing Penrose processes leading to the most intense possible jet.

## 5 Other characteristics

We remark that the study of the characteristics (21) of the system of equations (17) and (18) can produce other types of asymptotes. For example the characteristics in the first quadrant defined by

$$S = 0, \quad (38)$$

(i.e.  $\theta = \text{constant}$ ) have

$$\frac{dz}{d\rho} = \frac{(\alpha^2 - A)z}{\alpha^2 \rho}. \quad (39)$$

In the limit  $\rho, z \gg \sqrt{A}$ , (39) gives

$$\frac{dz}{d\rho} \approx \frac{z}{\rho}, \quad (40)$$

which together with  $S = 0$  implies that for an outgoing particle with  $L_z = 0$  and  $\mathcal{Q} < 0$

$$\frac{\rho}{z} \approx \left[ \frac{a^2(E^2 - 1)}{|\mathcal{Q}|} - 1 \right] \quad (41)$$

asymptotically. The asymptotic limit, in the meridional plane, is described by two straight lines crossing at the origin and defining in space a cone with aperture  $\theta$ . This will be as narrow as the slope,  $\theta \approx \rho/z$ , if  $z/\rho$  becomes big, which means that the lines become more vertical. This happens when

$$a^2(E^2 - \delta) - |\mathcal{Q}| \ll |\mathcal{Q}|, \quad (42)$$

and then  $\theta \ll 1$ . These asymptotes allow us to define another type of jet which is bigger and less collimated than the previous ones. It is interesting to remark that recent observations (Sheth et al., 2003; Sauty et al., 2002) suggest the existence of two different types of jets precisely of these sorts, i.e. narrowly and broadly collimated, as described in sections 3 and 5 respectively.

There exists an ensemble of geodesics that tend asymptotically to these conical characteristics. The unbounded geodesics have mainly been discussed, however, by using Boyer-Lindquist coordinates  $r$  and  $\theta$  by the majority of authors. If we rewrite our results, using these coordinates, we may interpret our results and compare to those of other authors. However, as we show below, these coordinates are not as well-suited to the issues we have discussed.

Geodesics with  $L_z \neq 0$  may reach low values of  $\rho/z$ , if  $b_2$  is large enough, but must be bounded away from  $|\cos\theta| = 1$  (i.e.  $\theta = 0$  or  $\theta = \pi$ ), since those values would imply  $\dot{\theta}^2 < 0$ , from (3), cf. Chandrasekhar (1983), p. 348. In practice this means that a jet along the axis must be composed of particles with very small  $L_z$ . Particles with non-zero  $L_z$  could only lie within a jet with bounded  $\rho$  for a limited distance, because large enough  $z$  would imply  $\dot{\theta}^2 < 0$ . If  $\mathcal{Q} \geq 0$ , the orbits reverse the sign of  $\dot{\theta}$  and reach the equatorial plane, and would thus be expected to be absorbed by the accretion disk. For  $\mathcal{Q} < 0$  they are confined to a band of values of  $\theta$  given by the roots of  $S^2 = 0$ . These are the ‘vortical’ trajectories of de Felice et al. (de Felice & Calvani, 1972; de Felice & Curir, 1992; de Felice & Carlotto, 1997). Depending on the maximum opening angle  $\theta$ , these may still hit, and presumably be absorbed by, a thick accretion disk (de Felice & Curir, 1992). Such orbits can be adequately populated by Penrose-like processes (Williams, 1995, 2004), and might undergo processes which reduce the opening angle (de Felice & Curir, 1992; de Felice & Carlotto, 1997). A jet composed of such particles would tend to be hollow and would have a larger radius  $\rho$  at large  $z$  than is obtained for orbits with  $L_z = 0$ . The presence of these escaping trajectories spiralling round the polar axis can be associated with the gravitomagnetic effects due to the rotation of the hole, one of whose consequences is that even curves with  $L_z = 0$  have a non-zero  $d\phi/dt$  at finite distances.

Thus although an infinitely extended jet of bounded  $\rho$  radius would only contain particles with  $L_z = 0$ , which we would expect to be a set of measure zero among all particles ejected, we shall take this as the right model even for real jets. In practice, interactions with other forces and objects, which would affect the jet both by gravitational and other forces, have to be taken into account once the jet is well away from the BH, and these influences might or might not improve the collimation. de Felice & Carlotto (1997) have discussed possible improved collimation for particles of low  $L_z$  using forces which have a timescale long compared with the dynamical timescale

of the geodesics, and which act to move particles to new geodesics with changed parameters. It should be noted that if the object producing the jet is modelled as a rotating black hole, production of a collimated jet only arises naturally if the object throws out energetic particles with low  $L_z$ , since our discussion shows that other particles cannot join such a jet unless there is some other strong collimating influence away from the BH.

However previous authors have not pointed out the existence of asymptotes  $\rho = \rho_1$ , presumably because they are less obvious when using coordinates  $r$  and  $\theta$ . In fact, considering  $z \rightarrow \infty$ , the expressions (12) and (15) produce  $\cos \theta \approx 1 - (\rho_1^2/2z^2) + O(z^{-3})$ ,  $\sin \theta \approx (\rho_1/z) + O(z^{-4})$  and  $r \approx z + 1 + (\rho_1^2/2z^2) + O(z^{-3})$ . With these expansions it is clear that in the limit  $\theta = 0$  one would have to take the limit of  $r \sin \theta$  to allow  $\rho_1$  to be determined.

In the same vein, to find the values of asymptotes  $z = z_1 \neq 0$  near the equatorial plane  $\theta = \pi/2$  for the incoming particles (see (37)) one has to study  $r \cos \theta$  if one uses the coordinates  $r$  and  $\theta$ . In fact, one finds for the asymptotic expansion  $\rho \rightarrow \infty$  the following expressions,  $\cos \theta \approx (z_1/\rho) + O(\rho^{-3})$ ,  $\sin \theta \approx 1 - (z_1^2/2\rho^2) + O(\rho^{-3})$  and  $r \approx \rho + 1 + [z_1^2 + 1 - (a/M)^2]/2\rho + O(\rho^{-3})$ .

Note that the geodesics studied here (in sections 3 to 5) do not exhaust all possible unbounded geodesics, or all characteristics of the system of equations producing the geodesics.

## 6 Penrose process and plotting of geodesics

Our model assumes that incoming particles arrive in the ergosphere and undergo a Penrose process. As mentioned earlier, in its original version (Penrose, 1969), each particle may be decomposed into two subparticles and one of them may cross the horizon and fall irreversibly into the BH, while the other is ejected to the exterior of the ergosphere; or the incoming particle may collide with another particle resulting in one plunging into the BH and the other being ejected to the exterior. The first case can correspond to a creation of particles, say  $e^-$  and  $e^+$  from a photon  $\delta = 0$ . We do not present here all the possible cases, which are exhaustively studied, especially for AGN, in Williams (1995, 2004). There is also observational evidence for a close correlation between the disappearance of the unstable inner accretion disk and some subsequent ejections from microquasars such as GRS 1915+1105 (Mirabel & Rodriguez, 1994, 1999). Here we are mainly interested in the

outgoing particles which follow geodesics that tend asymptotically towards a parallel to the  $z$  axis, as described in the previous section 3. These events are closely dependent on the possibilities allowed by the conservation equations. In the case when the incoming particle splits into two (Rees et al., 1976), the conservation equations of the energy and angular momentum are

$$E_{in} = E_{out} + E_{fall}, \quad (43)$$

$$L_{z,in} = L_{z,out} + L_{z,fall}. \quad (44)$$

We know from (24) that for the outgoing particles we study  $L_{z,out} = 0$ . The particles falling irreversibly into the BH have energy  $E_{fall}$  and angular momentum  $L_{z,fall}$ . The energy and the angular momentum of a particle in the ergoregion can be negative which is the basis of the Penrose process. The particle falling into the black hole has negative energy, and hence the outgoing particle, leaving the ergosphere, has a bigger energy than the incoming particle,

$$E_{out} = E_{in} + |E_{fall}|. \quad (45)$$

We have plotted numerically the geodesics for incoming, outgoing and falling particles with the following values for the parameters:  $a/M = 1/2$ ,  $E_{in} = 200$ ,  $E_{out} = 202$ ,  $E_{fall} = -2$ ,  $L_{z,in} = L_{z,fall} = -100$  and  $\mathcal{Q} = \mathcal{Q}' = 10^5$ . These values are chosen in such a way that the geodesics meet inside the ergoregion situated in the interior of the ergosphere

$$z^2 = \left\{ 1 - (\rho_e)^2 \left[ 1 - \left( \frac{\rho}{\rho_e} \right) \right] \right\} \left[ 1 - \left( \frac{\rho}{\rho_e} \right) \right], \quad (46)$$

and they produce for the asymptotes of the outgoing particles  $\rho_1 = 1.64341$  and for the incoming  $z_1 = 1.58116$ . The curves are built with the initial conditions  $z[1.55] = 20$  for outgoing particles and  $z[0.25] = 0.60$  for incoming particles. Their intersection is situated at the point  $\rho_i = 0.23$  and  $z_i = 0.59$  inside the ergosphere which we can take as the initial condition for the falling particle and from where we trace the three curves (see fig. 4).

The exhibition of these numerical solutions with outgoing geodesics with vertical asymptote with the value  $\rho_1$  precisely equal to (35) with (39) which leaves the ergosphere after the Penrose process, confirms the model presented.

## 7 Conclusion

Our main results are the following.

There are projections of geodesics all over the meridional planes. Among these geodesics there are some called type I, with vertical asymptotes parallel to  $z$ , that can represent jets. There are, as well, geodesics, called type II, with horizontal asymptotes parallel to the radial coordinate  $\rho$ , that can represent the paths of incoming particles leaving the accretion disk.

These two types of geodesics have intersection points that can be situated inside the ergosphere. At these points a Penrose process can take place, producing the ejection of particles of type I with bigger energies than the energies of incoming particles of type II. The energies of outgoing particles are significantly larger than the ones of the incident particles for the asymptotically vertical geodesics near the scale  $a/M$  of the ergosphere diameter in the coordinate  $\rho$ , explaining the almost perfect collimation along a tube of diameter  $2a/M$  centred on the axis of symmetry. These collimated outgoing particles have to have a zero orbital momentum  $L_z = 0$ , which implies, from the Penrose process, that the incoming particles have a negative orbital momentum,  $L'_z < 0$ . Thus the jet is fed from incoming particles with retrograde orbits in the accretion disk. There is evidence for the existence of substantial counterrotating parts of accretion disks (Koide et al., 2000; Thakar et al., 1997), and such counterrotations could explain the viscosity inducing the instabilities which trigger the falling of matter towards the ergosphere. It is now known (Mirabel & Rodriguez, 1994, 1999; Mirabel, 2006) that there is a close connection between instabilities in the accretion disk and the genesis of jets for quasars and microquasars.

The most energetic incoming particles are those near the equatorial plane. Hence the incoming particles which produce the most energetic outgoing particles by a Penrose process in the ergosphere, whose maximum size is  $z_e = \sqrt{A}$ , are those with angular momentum  $L'_z < 0$  and a very small impact parameter  $z_1$ .

Also, the limiting diameter of the jet depends upon the size of the ergosphere. The effective thickness of the jet in this case is of the order of  $2\rho_e = 2a/M$ .

The model that we present to explain the formation and collimation of jets arises essentially from relativistic strong gravitational field phenomena without the need to resort to electromagnetic phenomena.

Our model is sufficiently general to fit various types of observed jets, like GRB, jets ejected from AGN or from microquasars, whenever they are energetic enough to be explained by just a rotating black hole fed by an accretion disk in an axisymmetric configuration.

The existence of vacuum solutions of the Einstein equations of Kerr type but with a richer, not connected, topological configuration of the ergosphere (see Gariel et al. (2002), figs. 7 to 10), allows us to propose the existence of double jets, because they are expected to come out from the ergosphere. These bipolar jets have been observed (see for instance Skinner et al. (1997), Sahai et al. (1998) fig. 1, Fargion (2003) fig. 2, and Kwok et al. (1998)) and could be naturally interpreted in a generalization of our model.

**Acknowledgement** We are grateful to Dr. Reva Kay William for correspondence concerning her papers and for further references.

## References

Blandford R., Znajek R., 1977, Mon. Not. R. Astron. Soc., 179, 433

Carter B., 1968, Phys. Rev., 174, 1559

Chandrasekhar S., 1983, The Mathematical Theory of Black Holes. Oxford University Press, Oxford

de Felice F., Calvani M., 1972, Nuovo Cimento B, 10, 447

de Felice F., Carlotto L., 1997, Astrophys. J, 481, 116

de Felice F., Curir A., 1992, Class. Quantum Grav., 9, 1303

de Felice F., Zanotti O., 2000, Gen. Rel. Grav., 32, 1449

Fargion D., 2003, astro-ph/0307314, Puzzling afterglow's oscillations in GRBs and SGRs: tails of precessing jets

Gariel J., Marcilhacy G., Santos N., 2002, Class. Quantum Grav., 19, 2157

Herrera L., Santos N., 2005, gr-qc/0505074 v1, A general relativistic effect in quasi-spherical objects as the possible origin of relativistic jets

Hughston L., Penrose R., Sommers P., Walker M., 1972, Commun. math. phys., 27, 303

Koide S., Meier D., Shibata K., Kudoh T., 2000, Astrophys. J., 536, 668

Kwok S., Su K., Hrivnak B., 1998, Astrophys. J., 501, L117

Livio M., 1999, *Phys. Rep.*, 311, 225

McClintock J., Shafee R., Narayan R., Remillard R., Davis S., Li L.-X., 2006, *Astrophys. J.*, 652, 518

McKinney J., 2005, astro-ph/0506368 v1, Jet formation in black hole accretion systems I: theoretical unification model

Mirabel I., 2006, astro-ph/0612188, Black holes: from stars to galaxies

Mirabel I., Rodriguez L., 1994, *Nature*, 371, 46

Mirabel I., Rodriguez L., 1999, *Ann. Rev. Astr. Astrophys.*, 37, 409

O'Neill B., 1995, *The Geometry of Kerr Black Holes*. A K Peters Ltd., Wellesley, Massachusetts

Opher R., Santos N., Wang A., 1996, *J. Math. Phys.*, 37, 1982

Penrose R., 1969, *Rivista del Nuovo Cimento*, Numero Special, 1, 252

Piran T., Kumar P., Panaitescu A., Piro L., 2001, *Astrophys. J.*, 560, L167

Piran T., Shaham J., 1977, *Phys. Rev. D*, 16, 1615

Punsly B., 2001, *Black Hole Gravitohydromagnetics*. Springer-Verlag, Berlin and Heidelberg

Punsly B., Coroniti F., 1990a, *Astrophys. J.*, 354, 583

Punsly B., Coroniti F., 1990b, *Astrophys. J.*, 350, 518

Rees M., Ruffini R., Wheeler J., 1976, *Black Holes, Gravitational Waves and Cosmology: An Introduction to Current Research*. Gordon and Breach Science Publishers, New York

Sahai R., Trauger J., Watson A., Stapelfeldt K., Hester J., Burrows C., Bally J., Clarke J., Crisp D., Evans R., Gallagher J., Griffiths R., Hoessel J., Holtzman J., Mould J., Scowen P., Westphal J., 1998, *Astrophys. J.*, 493, 301

Sauty C., Tsinganos K., Trussoni E., 2002, in Guthmann A., Georganopoulos M., Marcowith A., Manolakou K., eds, Springer Lecture Notes in Physics, Vol. 589, Relativistic Flows in Astrophysics. Springer-Verlag, Berlin and Heidelberg, p. 41

Sheth K., Frail D., White S., Das M., Bertoldi F., Walter F., Kulkarni S., Berger E., 2003, *Astrophys. J.*, 595, L33

Skinner C., Meixner M., Barlow M., Collison A., Justtanont K., Blanco P., Pina R., Ball J., Keto E., Arens J., Jernigan J., 1997, *Astron. and Astrophys.*, 328, 290

Thakar A., Ryden B., Jore K., Broeils A., 1997, *Astrophys. J.*, 479, 702

Wilkins D., 1972, *Phys. Rev. D*, 5, 814

Williams R., 1995, *Phys. Rev. D*, 51, 5387

Williams R., 2004, *Astrophys. J.*, 611, 952